

# OPTICAL OBSERVATION OF HYDROGEN AND DEUTERIUM CRYSTAL GROWTH AND IMPLICATIONS FOR ULTRACOLD NEUTRON TRANSMISSION EXPERIMENTS

Stefan Döge (Doege)<sup>1,2,3</sup>, Jürgen Hinger<sup>1,2</sup>, Christoph Morkel<sup>1</sup>, Bernhard Lauss<sup>4</sup>, Nicolas Hild<sup>4,5</sup>, Tobias Jenke<sup>2</sup>

<sup>1</sup> Physik Department, Technische Universität München (TUM), Garching, Germany

<sup>2</sup> Institut Laue-Langevin (ILL), Grenoble, France

<sup>3</sup> Université Grenoble Alpes (UGA), Saint-Martin-d'Hères, France

<sup>4</sup> Laboratory for Particle Physics, Paul Scherrer Institut (PSI), Villigen, Switzerland

<sup>5</sup> Institute for Particle Physics, ETH Zürich, Zürich, Switzerland

## Abstract

The precise knowledge of UCN cross sections in solid deuterium is pivotal to the design and improvement of new UCN sources, which promise to provide higher UCN densities than the long-time frontrunner – the "turbine" at Institut Laue-Langevin (ILL) in Grenoble, France. However, previous experimental results in this field have been distorted by UCN scattering on rough surfaces and have not been able to describe the size and concentrations of defects present in solid deuterium. In this paper we present a new sample container with highly polished silica windows that eliminate UCN scattering on rough sample surfaces. Preliminary experimental results for UCN scattering cross sections in liquid and solid deuterium are shown. The size and concentration of defects in the deuterium crystals are estimated using the Guinier model.

Key words: cryogenic seal, neutron scattering, optical properties, ultracold neutrons

## I. Introduction

Ultracold neutrons (UCNs) are a versatile tool for fundamental physics experiments, such as the exact determination of the free-neutron lifetime [1], the search for a possible non-zero neutron electric dipole moment [2] and other aspects important to cosmology, quantum mechanics and particle physics [3]. It is common to all these experiments that their statistics would be considerably improved, if stronger UCN sources were available.

Superthermal UCN converters [4] based on superfluid helium and solid deuterium ( $sD_2$ ), see for example [5,6,7], promise higher UCN fluxes than the currently strongest continuously operating converter – the "turbine" at Institut Laue-Langevin (ILL) in Grenoble, France [8]. This promise has, however, only partially been kept. The output of operational UCN converters based on  $sD_2$  in pulse mode is more than an order of magnitude lower than initially predicted [9] and only the best one has a UCN density somewhat higher than that of the turbine [10]. This was the motivation for re-measuring the scattering cross sections of  $sD_2$  in the UCN and lower VCN energy range.

## II. Previous Experiments

To our knowledge, the first very cold neutron (VCN) transmission measurements on solid deuterium were done by a group at PNPI, Gatchina [11]. They froze out deuterium from the liquid phase at four different speeds (freezing time 20 min, 1 hour, 2 hours, 3 hours). It was expected to see an unambiguous correlation between freezing speed and VCN transmission. The slower the crystal was frozen, the more transparent for VCNs it should be. The results, however, painted a different, unclear picture, see Fig. 1.

One problem was that the sample container was made from machined (unpolished) titanium. The amount of surface scattering on the container windows could not be quantified. It was equally impossible to optically verify both the fill height of the liquid in the sample container and the uniform freezing of the solid. Instead, the fill level was inferred from the container volume and the pressure difference in the gas reservoir. Therefore, the exact sample thickness was not well known. Also, it is possible that part of the liquid froze out on the walls of the sample container above the liquid level, thereby reducing the sample thickness. The VCN transmission was measured vertically.

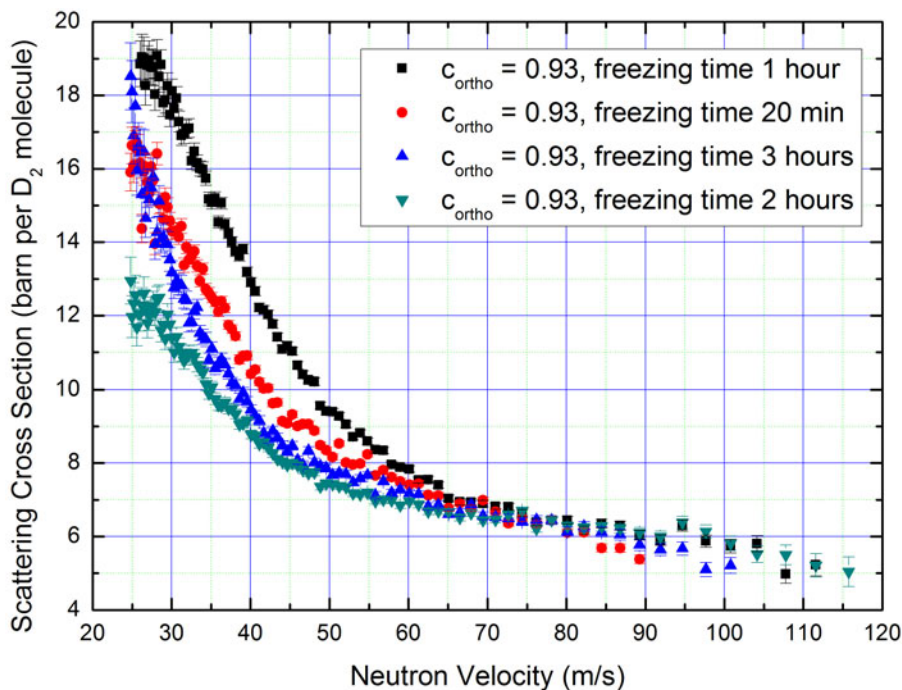


Figure 1. Scattering cross sections for solid deuterium crystals of various freezing speeds as inferred from VCN transmission [11].

The only other direct slow-neutron transmission experiments on deuterium that we are aware of, were carried out by a group from Paul Scherrer Institut in Switzerland [12,13] who used UCNs and VCNs. These experimenters employed an aluminum sample container with neutron windows made from machined aluminum AlMg3. During the experiments these windows bulged due to pressure differentials and introduced an error to the cross sections of about 10%. The final results were modeled using an effective sample thickness. The crystals could be observed laterally through a sapphire window. Photos from [13] suggest cracks being

present in the crystals frozen from the liquid phase. The rough surfaces of the aluminum windows, and consequently also the rough surfaces of the deuterium crystals, attenuated the UCN beam by an unquantified magnitude.

### III. Experimental Setup

Total UCN cross sections of hydrogen and deuterium were determined in transmission geometry with a time-of-flight (TOF) setup using collimated UCNs, see Fig. 2. The measured transmitted UCN flux through the filled and empty sample containers can be related to the total cross section by Equations 1 and 2:

$$\frac{I_{\text{filled}}}{I_{\text{vacuum}}} = e^{-\Sigma_{\text{tot}}d} = e^{-\sigma_{\text{tot}}N_Vd} \quad (1) \quad \sigma_{\text{tot}} = \frac{1}{N_Vd} \ln\left(\frac{I_{\text{vacuum}}}{I_{\text{filled}}}\right), \quad (2)$$

where  $I$  is the UCN count rate at the detector (with the subscript *vacuum* for vacuum in the sample cell and *filled* with a sample),  $d$  is the sample cell thickness, and  $N_V$  the molecular number density of the sample. The condition  $\Sigma_{\text{tot}}d < 1$  must be met in order to reduce multiple scattering and not to distort the *single*-scattering cross section, which is measured.

The scattering cross section was obtained by subtracting from the total cross section the absorption cross section of hydrogen and deuterium, respectively, which obeys a  $1/v$  behavior from thermal neutron energies down to the UCN range.

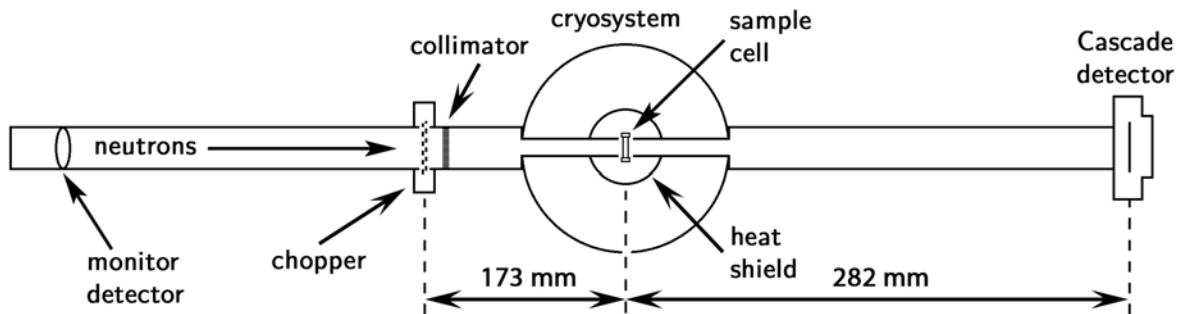


Figure 2. Time-of-flight (TOF) setup used to obtain the experimental results reported in this article.

For the first time, the deuterium crystals and liquids were measured in a sample container with highly polished ( $R_a < 3$  Ångström) and optically transparent windows made from amorphous silica [15], see Fig. 3. This reduced UCN surface scattering [16] to a minimum and allowed for proper online observation of the sample along the beam axis prior to the transmission measurement with UCNs. The sample container was mounted directly onto the cold-head of a closed-cycle helium refrigerator and was used in the same cryostat described in [17].

The key advantages of the new sample container over previous containers using aluminum neutron windows were:

- well defined sample thickness with an uncertainty of  $\sim 0.05$  mm over the entire sample area
- highly polished ( $R_a < 3 \text{ \AA}$ ) and thin ( $d = 1.0$  mm) amorphous silica windows, which do not show any small-angle scattering [18]
- optically transparent windows with a low neutron-optical potential (90 neV for amorphous  $\text{SiO}_2$ ) and of high purity (no scattering length density inhomogeneities in the material)
- vacuum seal that is hydrogen-tight down to 4.5 K

The *para/ortho*-deuterium concentration was monitored before and after each UCN measurement run by Raman spectroscopy. The main results were obtained for  $c_{\text{ortho}} = 0.982 \pm 0.002$ . Details on the nuclear spin and rotational states (species) of deuterium are given in [17] and a comprehensive review of hydrogen and deuterium properties was published in [19].



*Figure 3. Copper sample container with transparent amorphous silica ( $\text{SiO}_2$ ) windows used to obtain the UCN scattering cross sections presented in Section V.*

The new sample container itself is described in detail in [20].

#### **IV. Observations at Cryogenic Temperatures**

After the first condensation trials it became clear that it was not possible to freeze a crystal from the gaseous phase in our sample container. Therefore, we focused on producing transparent hydrogen and deuterium crystals from the liquid phase. The liquid was condensed into the sample container by keeping the container's temperature and the gas pressure at the

respective substance's triple point (deuterium: 18.7 K, 171.3 mbar [21]). Within a few minutes, the container was completely filled with liquid while a solid layer had already started forming from the bottom and the side walls of the container. Since the container body was made out of copper, it was well thermalized to the cold-head temperature. Before the entire liquid reservoir became frozen, the gas inlet froze over and no additional liquid could enter the container to fill the space that was vacated during the liquid-to-solid phase transition.

In the case of deuterium, the density increases by 12%, that of hydrogen by 11% upon freezing [21]. This volume shrinkage resulted in the formation of bubbles that rose to the top of the unfrozen liquid reservoir, see Fig. 4 (b). As the freezing progressed radially inward, these bubbles were pushed towards the middle of the sample container. In the end, as almost all the liquid had frozen, the boundaries of the bubbles curled up and formed a phase than can best be called "snow", see Fig. 4 (c).

Since UCNs are very sensitive to surfaces and interfaces, see [14], it was clear that UCN transmission measurements through this snow would not yield any useful data. And that snow always ended up right in the center of the container and hence at the spot of the highest UCN flux. To remedy this problem, the snowy area was melted and refrozen by minimal temperature changes of a few 0.1 K, see Fig. 4 (d). After about ten melt-and-refreeze cycles, the snow had vanished and there remained only one void in the center of the container, see Fig. 4 (e, f).

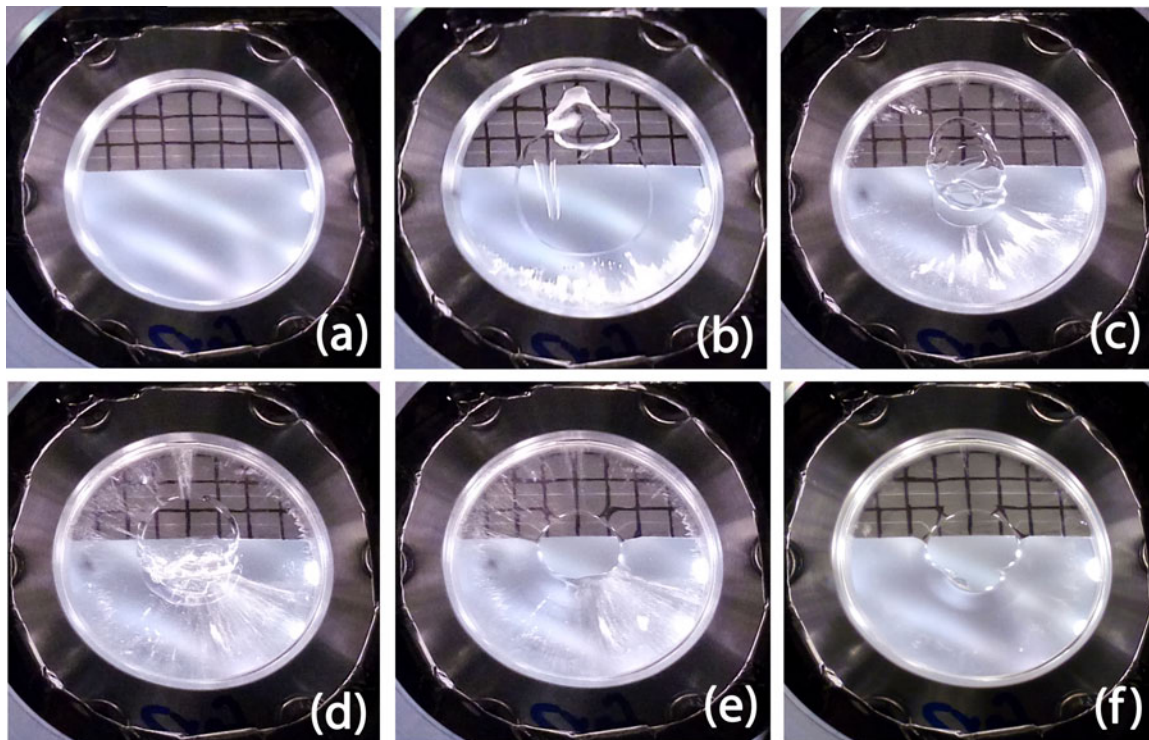


Figure 4. View of the sample container along the neutron beam axis as seen through the viewport and mirror. The upper part of the sample container is blinded out for ultracold neutrons by a 0.5 mm thick cadmium absorber. The marking lines on the absorbers are for reference and are 5 mm apart from each other. Picture (a) shows an empty sample container and (b-f) show liquid and solid para-hydrogen at various stages of freezing,  $d_{\text{sample}} = 4.5$  mm.

Picture (b) shows a liquid-filled para-hydrogen crystal ring with bubble formation in the liquid phase; (c) freshly frozen solid para-hydrogen, irregular solid–liquid–vacuum phase boundaries (“snow”) in the center of the sample container, visible radial streaks; (d) the previous crystal after one melt–refreeze cycle; (e) the previous crystal after about 10 melt–refreeze cycles, where the irregular phase boundaries have disappeared and a void with a smooth surface has formed; (f) the previous crystal after 15 hours at constant temperature ( $T = 9\text{ K}$ ) and one short melt–refreeze cycle, the radial marks have disappeared as they were located not in the crystal bulk, but only on the crystal–window interface.

After observing and learning about the process of bubble formation, we decided to use a flap-shaped 0.5 mm thick cadmium absorber to blind out that area of the UCN window, where the bubble would reliably form. Since that diminished the transmitted UCN flux considerably, the entire sample container was lifted up by placing a 9 mm thick aluminum disk between the cold-head and the sample container. This way, the highest UCN flux passed through the crystal area just below the cadmium absorber. In the end, all measurements on solid samples were done in this configuration, see Fig. 5.

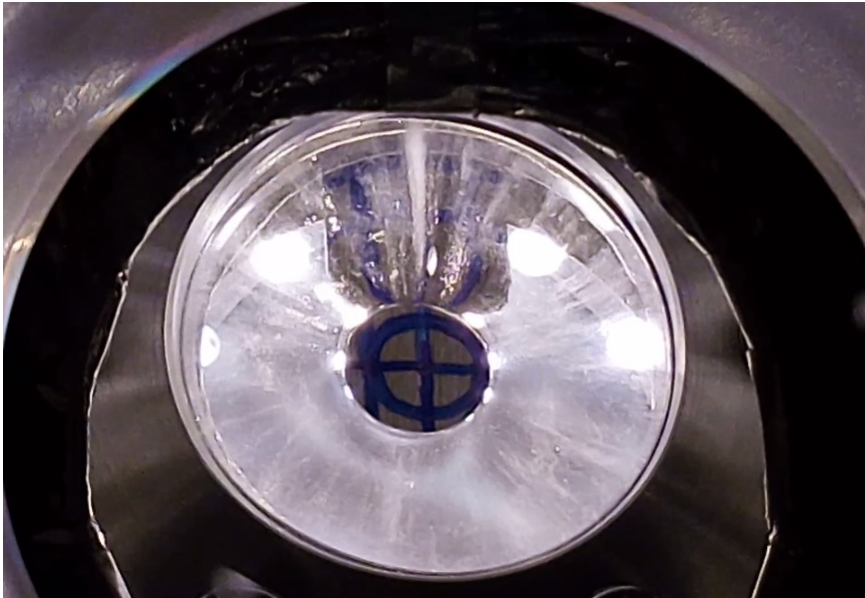


Figure 5. A frozen and temperature-cycled ortho-deuterium crystal ( $d_{\text{sample}} = 6.5\text{ mm}$ ) cooled to  $T = 10\text{ K}$  is shown. The central void (filled with deuterium gas at its corresponding vapor pressure) was blinded out by a 0.5 mm thick cadmium absorber for UCNs.

## V. Preliminary Experimental Results for Liquid and Solid Deuterium

The preliminary total cross sections (scattering plus absorption, corrected for reflection at the vacuum interface) of liquid *ortho*-deuterium ( $c_{\text{ortho}} = 0.98$ ) for UCNs are shown in Fig. 6. The experimental data for the temperatures 19.0 K, 20.6 K and 23.0 K overlap well with the model published in [17], which was calculated for the respective temperatures using the self-diffusion coefficient of liquid deuterium from O'Reilly et al. [22] and Guarini et al. [23].

The temperature uncertainty for the experimental data was  $\pm 0.2\text{ K}$ . The new experimental data on liquid deuterium should be seen as an improvement (and replacement) of the *experimental*

data published in [17] and [24].

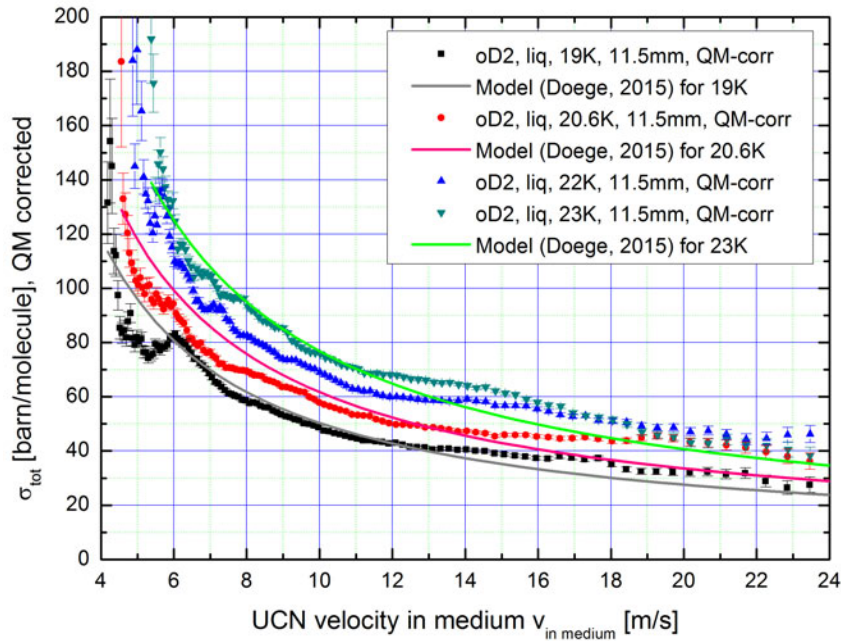


Figure 6. Preliminary experimental data (solid colored symbols) for the total cross section of liquid *ortho*-deuterium at various temperatures. The theoretical model [17] was calculated for  $T = 19\text{ K}/20.6\text{ K}/23.0\text{ K}$  at  $c_{ortho} = 0.98$  (solid colored lines).

The preliminary total cross sections (scattering plus absorption, corrected for reflection at the vacuum interface) of solid *ortho*-deuterium ( $c_{ortho} = 0.98$ ) for UCNs are shown in Fig. 7. The black squares represent *normal*-deuterium at 15 K. Below them, the red circles represent solid *ortho*-deuterium at 10 K and the green down triangles stand for the same crystal at 14.5 K. The blue up triangles stand for the same crystal after the temperature cycling 10 K/ 14.5 K/ 10 K. It is clear that temperature cycling does not lower the scattering cross section of a crystal. In the best case, it remains the same. Qualitatively similar findings were published in [12,13]. In the particular case shown here, the cross section increased slightly as a result of temperature cycling. The red dots from Fig. 8 (solid *ortho*-deuterium at 10 K) are plotted again in Fig. 8. There, they are decomposed into their constituents: 1-phonon up-scattering, incoherent elastic nuclear scattering and elastic scattering contributions from defects ( $R_d = 88\text{ \AA}$ ,  $c = 8.2 \times 10^{-11}$  per  $D_2$  molecule) as calculated using the Guinier approximation [25]. This is the first time that an estimation of the size and concentration of defects in deuterium crystals was done for the purposes of UCN scattering.

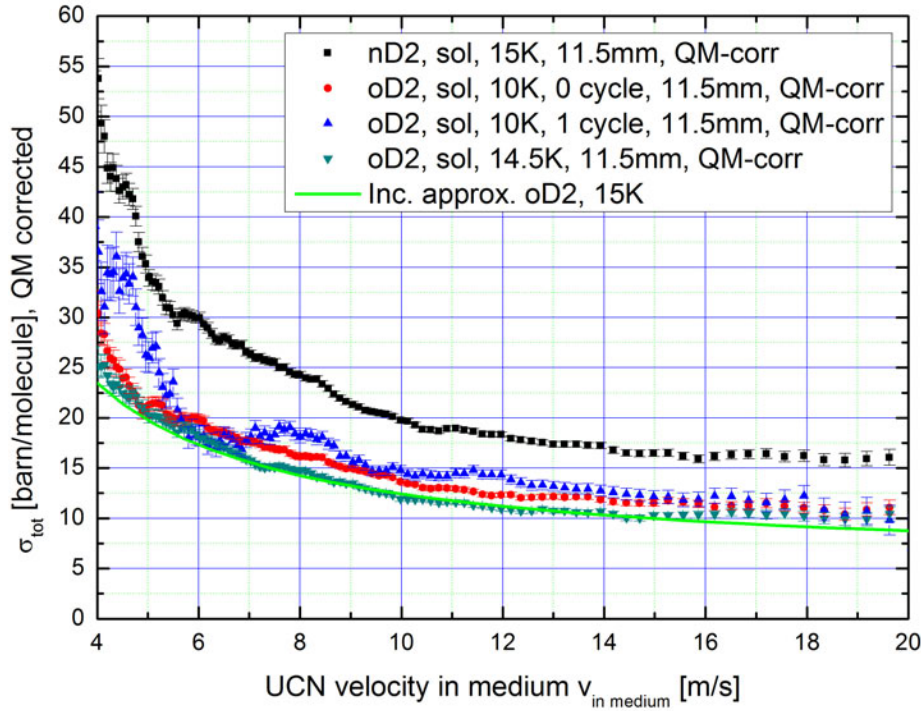


Figure 7. Preliminary experimental data for solid normal- and ortho-deuterium at  $T = 10$  K and  $15$  K and after no and after one temperature cycling. The theoretical model (incoherent approximation for 1-phonon up-scattering, solid green line) was calculated for  $T = 15$  K.

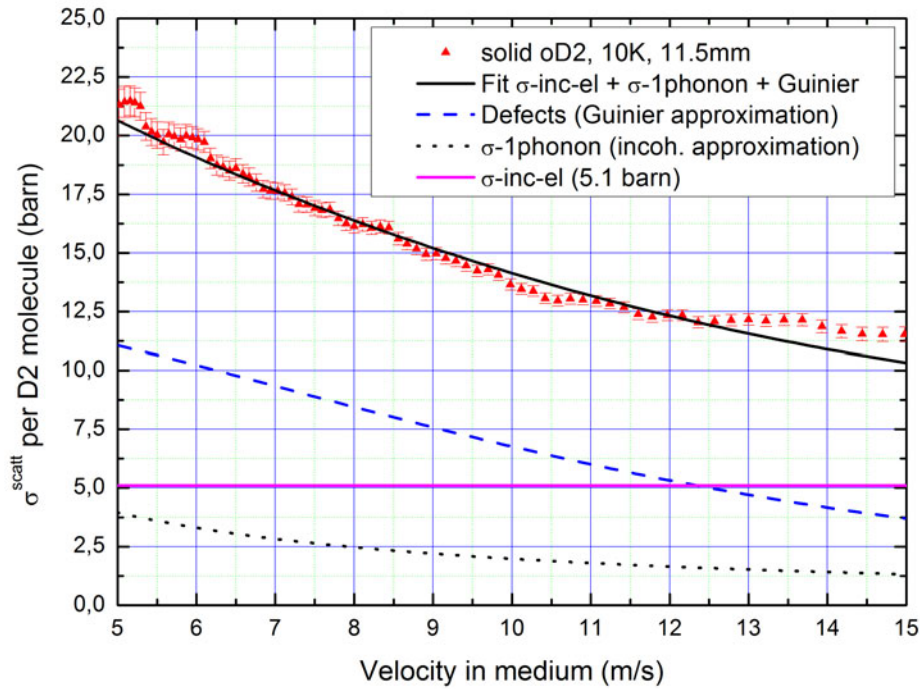


Figure 8. Preliminary total scattering cross section of solid ortho- $D_2$  ( $T = 10$  K) and its decomposition into 1-phonon up-scattering, incoherent elastic nuclear scattering and the elastic scattering contributions from defects ( $R_d = 88$  Å,  $c = 8.2 \times 10^{-11}$  per  $D_2$  molecule) as calculated using the Guinier approximation [25].

## VI. Conclusion

We have conceived, constructed and tested a sample container for cryogenic liquids and solids that produces samples with low surface roughness and allows for optical inspection of the sample preparation process. The highly polished silica windows suppress surface scattering as much as possible and do not bulge under pressure. This sample container design addresses the issues of previous sample containers and permits reliable UCN transmission measurements on cryogenic crystals, such as solid deuterium ( $sD_2$ ). Measurements of this kind are needed to interpret the performance of operating  $sD_2$ -based UCN sources worldwide.

We have used this sample container in recent UCN transmission measurements and were able to determine precise total cross sections of liquid and solid *ortho*-deuterium for UCNs and determine the concentration of defects in an *ortho*-deuterium crystal.

## Acknowledgment

The authors are sincerely grateful to ILL and TU Munich technical staff, especially to O. Losserand, E. Bourgeat-Lami, T. Brenner, D. Berruyer and P. Hartung for advice on cryogenics, technical drawings and producing parts of the experimental equipment. A. Frei and T. Lauer of Forschungsneutronenquelle Heinz Maier-Leibnitz (FRM-II) and P. Geltenbort of ILL are acknowledged for lending experimental equipment and giving useful advice.

The authors thank Forschungsneutronenquelle Heinz Maier-Leibnitz (FRM-II) at Technische Universität München, Germany, and Leonhard-Lorenz-Stiftung Munich, Germany, who contributed financially to this project.

## References

- [1] C. Patrignani and others (Particle Data Group). 2017 review of particle physics. *Chin. Phys. C* **40**, 100001 (2016 and 2017 update). URL: <http://pdg.lbl.gov>.
- [2] P. Schmidt-Wellenburg. The quest for an electric dipole moment of the neutron. *AIP Conference Proceedings* **1753**(1), 060002 (2016).
- [3] D. Dubbers and M.G. Schmidt. The neutron and its role in cosmology and particle physics. *Rev. Mod. Phys.* **83**, 1111–1171, (2011).
- [4] R. Golub and J.M. Pendlebury. Super-thermal sources of ultra-cold neutrons. *Physics Letters A* **53**(2), 133–135 (1975).
- [5] O. Zimmer et al. *Phys. Rev. Lett.* **107**, 134801 (2001).
- [6] B. Lauss, Ultracold neutron production at the second spallation target of the Paul Scherrer Institute, *Physics Procedia* **51**, 98 (2014).
- [7] A. Saunders et al. *Review of Scientific Instruments* **84**, 013304 (2013).
- [8] ILL 2017.  
URL: <http://www.ill.eu/instruments-support/instruments-groups/instruments/pf2/>
- [9] F. Atchison et al. Investigation of solid  $D_2$ ,  $O_2$  and  $CD_4$  for ultracold neutron production. *Nuclear Instruments and Methods A* **611**, 252 (2009).
- [10] D. Ries et al. *Phys. Rev. C* **95**, 045503 (2017).

- [11] A.P. Serebrov et al. *Pis'ma ZhETF* **74**, 6, 335-338 (2001).
- [12] F. Atchison et al. *Phys. Rev. Lett.* **95**, 182502 (2005).
- [13] T. Brys, PhD thesis, ETH Zurich (2008).
- [14] W.-D. Seiffert, PhD thesis TU Munich (1969) and Euratom Report No. EUR 4455 d (1970).
- [15] J.S. Laufer, *J. Opt. Soc. Am.* **55**, 458 (1965).
- [16] Steyerl, A., *Z. Phys.* **254**, 169 (1972).
- [17] S. Döge (Doege) et al. Scattering cross sections of liquid deuterium for ultracold neutrons: Experimental results and a calculation model. *Phys. Rev. B* **91**, 214309 (2015), also pre-print arXiv:1511.07065 [nucl-ex] (2015).
- [18] M. Roth. *J. Appl. Cryst.*, **10** (3), 172–176 (1977).
- [19] I.F. Silvera. The solid molecular hydrogens in the condensed phase: Fundamentals and static properties. *Rev. Mod. Phys.* **52**, 393–452, (1980).
- [20] S. Döge (Doege) and J. Hingerl, *Rev. Sci. Instrum.* **89**, 033903 (2018).
- [21] P.C. Souers. *Hydrogen Properties for Fusion Energy*. Univ. of California Press, Berkeley (1986).
- [22] D. E. O'Reilly and E. M. Peterson. Selfdiffusion of liquid hydrogen and deuterium. *Journal of Chemical Physics* **66**, 934 (1977).
- [23] E. Guarini et al. Velocity autocorrelation by quantum simulations for direct parameter-free computations of the neutron cross sections. II. Liquid deuterium. *Phys. Rev. B* **93**, 224302 (2016) and priv. comm.
- [24] S. Doege et al. ISINN-23 Conference Proceedings, JINR Dubna (Russia), pp. 119-130 (2016).
- [25] A. Guinier and G. Fournet, *Small Angle Scattering of X-Rays*. John Wiley, New York (1955).

